JOURNAL OF MATERIALS SCIENCE 32 (1997) 5985–5991

Abnormal grain growth of austenite in a V–Nb microalloyed steel

O. FLORES, L. MARTINEZ
Instituto de Física, Universidad Nacional Autonoma de Mexico. A. P. 48-3. C.P. 62251 Cuernavaca, Morelos, Mexico

An investigation was made of the grain-growth kinetics of the V–Nb microalloyed steel austenite phase at temperatures in the range 1173–1373 K, relevant for the understanding of the steel thermomechanical processing. The fine precipitation of vanadium- and niobium-rich particles plays an important role in helping the alloy to maintain a fine grain structure, which was characterized using optical microscopy, scanning electron microscopy and transmission electron microscopy. It was found that at temperatures where the fine precipitate particles are stable, the grain-growth process is slow and the mode of grain growth is normal. At higher temperatures where the precipitates are prone to dissolve, the abnormal grain-growth mode dominates. All the observations were comprised in a time–temperature map of the grain-growth modes. The map was built up by employing extensive line-intercept measurements of grain sizes at different temperatures and annealing times, followed by numerical calculations yielding curves of grain-growth rate as a function of grain size at different time intervals. The present experimental observations were found consistent with the results of calculations and predictions of the earlier theoretical work.

1. Introduction

The grain size is a major factor which determines mechanical, electrical and magnetic properties of materials. Grain growth occurs as a result of materials processing and gives rise to microstructural changes that determine the final grain-size distribution and the final properties of materials [1]. The driving force for grain growth is primarily the tendency to reduce the material's overall grain-boundary area. This grain-boundary area is the main source of energy for the grain-growth process [2].

Grain growth can occur in two modes: normal grain growth and abnormal grain growth. The two modes have been studied since the 1940s, employing theoretical and experimental approaches [3–13]. The characteristics of the normalized grain-size evolution, both with and without time invariance, are relevant for normal or abnormal grain growth. The evolution with time invariance shows a uniform increase in grain size and a steady-state kinetic process. It is accepted that for normal grain growth, the kinetic law is represented by $\bar{R} = kt^n$, where $\bar{R}$ is the average grain size, t the time, and k and n are material- and temperature-related constants. Abnormal grain growth (also known as secondary recrystallization), is characterized by the rapid increase of the largest grains at a rate much faster than the mean $\bar{R}$.

Elements such as vanadium, niobium and titanium have been employed to produce fine precipitation in order to inhibit austenitic recrystallization and grain growth. This is relevant for steels undergoing hot rolling, welded heat-affected zones or annealed and forged parts. Microalloying additions and appropriate thermomechanical processing are, in fact, the basis of the grain-refinement technology of steels. If grain-growth inhibition fails, the grain growth may become abnormal, producing a few larger grains [12, 14–17, 18–20]. This normal–abnormal grain-growth transition has been the topic of several studies [4, 7, 13, 16, 18–20]. In the normal grain-growth models, [3–5, 7, 19] the criterion for normal grain growth is established typically when the majority of grains are less than two to three times the mean size.

In this investigation, the kinetic behaviour of grain growth of a V–Nb microalloyed steel was studied and a comparison was made between the experimental results and some models of grain growth.

2. Experimental procedure

This investigation was carried out using an V–Nb microalloyed steel of 60 kgf mm^{-2} yield point, with the chemical composition given in Table I. The microalloyed steel was produced by a conventional sequence of blast furnace, basic oxygen furnace (BOF) ladle treatment and continuous casting process. Samples for chemical analysis were taken after adjusting the chemical composition during the ladle treatment. Billets of 125 mm of section, were reheated to 1423 K and rolled to obtain bars of 19 mm diameter. The temperature at the end of the rolling process was of the order of 1273 K. Samples for mechanical

0022–2461

characterization were taken from the bars and tested at room temperature. Cylindrical samples, 9 mm diameter and 9 mm high, were machined and subsequently annealed at 1123 K and cooled in stirred water to room temperature, in order to determine initial austenitic grain-size distribution. The samples were annealed during definite time intervals at three different temperatures and then they were quenched in agitated water. The samples were tempered at 723 K for 30 min after quenching. Heat treatments are shown in Table II.

After being tempered, the samples were cut through the middle in order to avoid the thick decarburized layer formed during annealing. Polishing was done using sand paper and 1 and 0.3 μm alumina powders. In order to evaluate austenite average grain size and grain-size distribution, the samples were further

TABLE I Chemical composition

Element	C	Mn	Si	P	S	Nb	V	N	Ni	Mo	Cr	Sb	Al
wt %	0.3	1.36	0.32	0.038	0.011	0.036	0.15	0.0053	0.012	0.042	0.013	0.008	0.004

TABLE II Heat treatments

Time (min)	1173 K	1273 K	1373 K
2	–	XX	XX
3	–	XX	XX
5	XX	XX	XX
10	XX	XX	XX
30	XX	XX	XX
60	XX	XX	XX
120	XX	XX	XX
480	XX	XX	XX

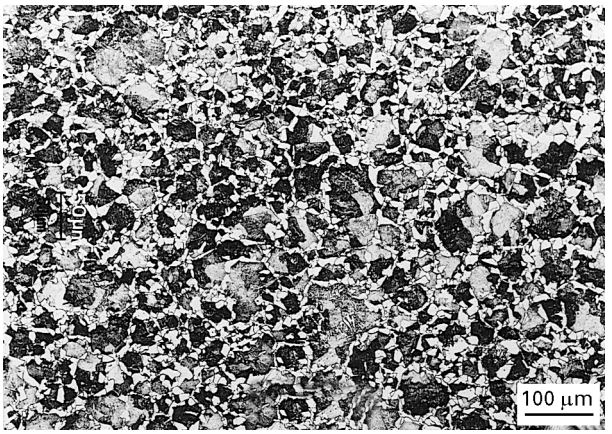

Figure 1 The fine-grained ferrite–pearlite microstructure of steel.

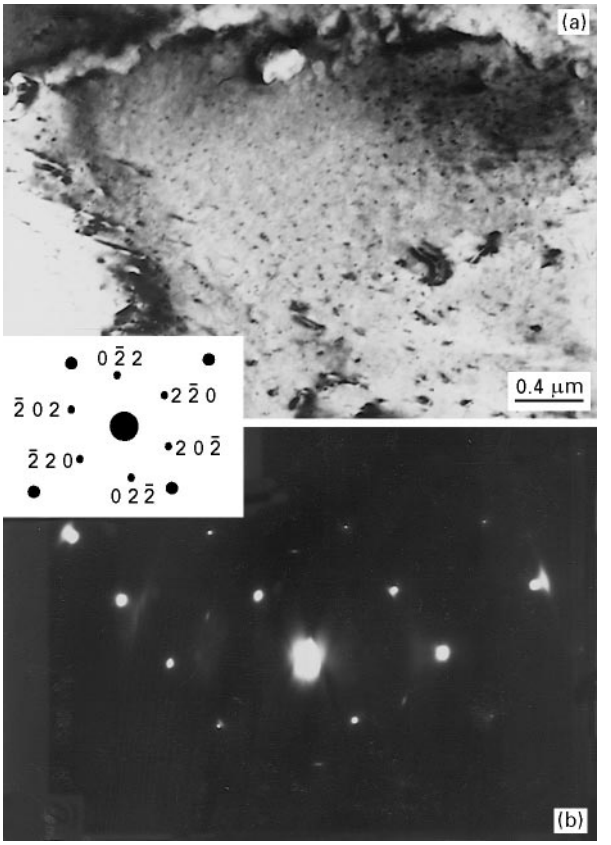

Figure 2 (a) A ferrite grain showing fine precipitation (bright field); (b) Diffraction pattern from the ferrite grain shown in (a).

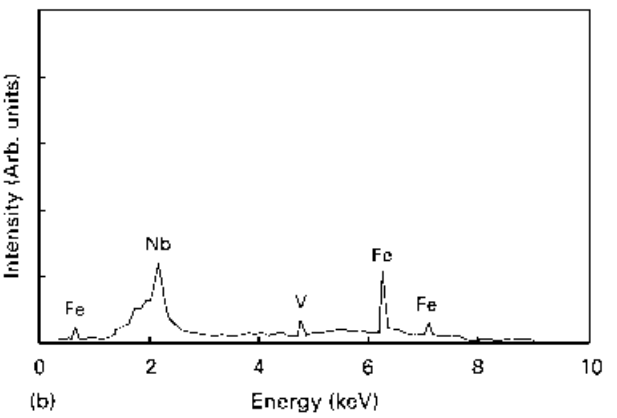

Figure 3 (a) Facetted precipitates with high niobium content; (b) EDS spectrum.

etched using a saturated aqueous picric acid solution, without wetting agent. Nital reagent (2% nitric acid in ethanol) was used to reveal the microstructure. Metallographic examination was carried out in samples from the as-received bars and also from the tempering conditions.

Observations were carried out in an Olympus PMG3 optical microscope, a Jeol CX 100kV transmission electron microscopy (TEM) and a JSM-T200 scanning electron microscope (SEM) with an energy dispersive spectroscopic (EDS) analyser. For the TEM observation, a thin foil was machined from samples. Discs, 3 mm diameter, were cut from the foil and etched in a twin-jet electropolishing machine using a 10% perchloric acid solution in ethanol.

The average grain size and grain-size distribution were determined employing the linear intercept method. Histograms in cumulative form were obtained using a minimum of 500 measurements in each sample. Because the grain size distributions could be closely fitted to log normal distribution in a cumulative form, this continuous expression was used instead

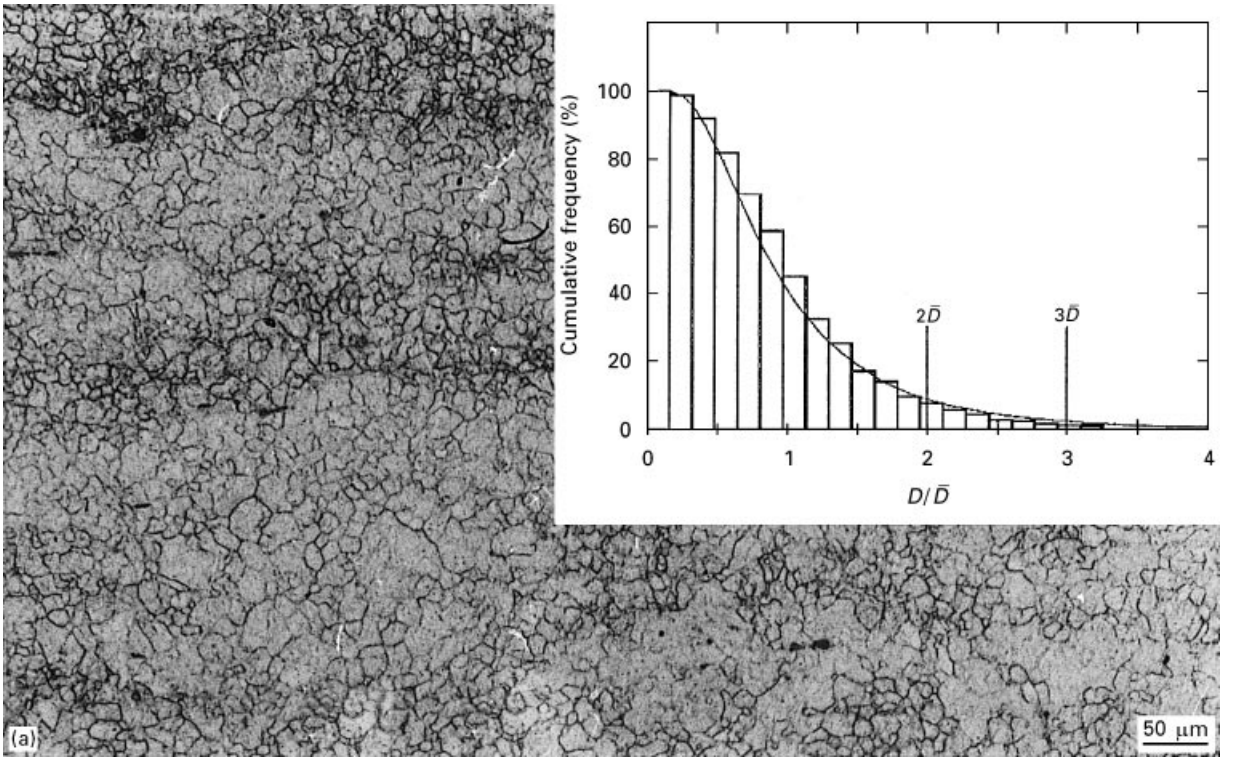

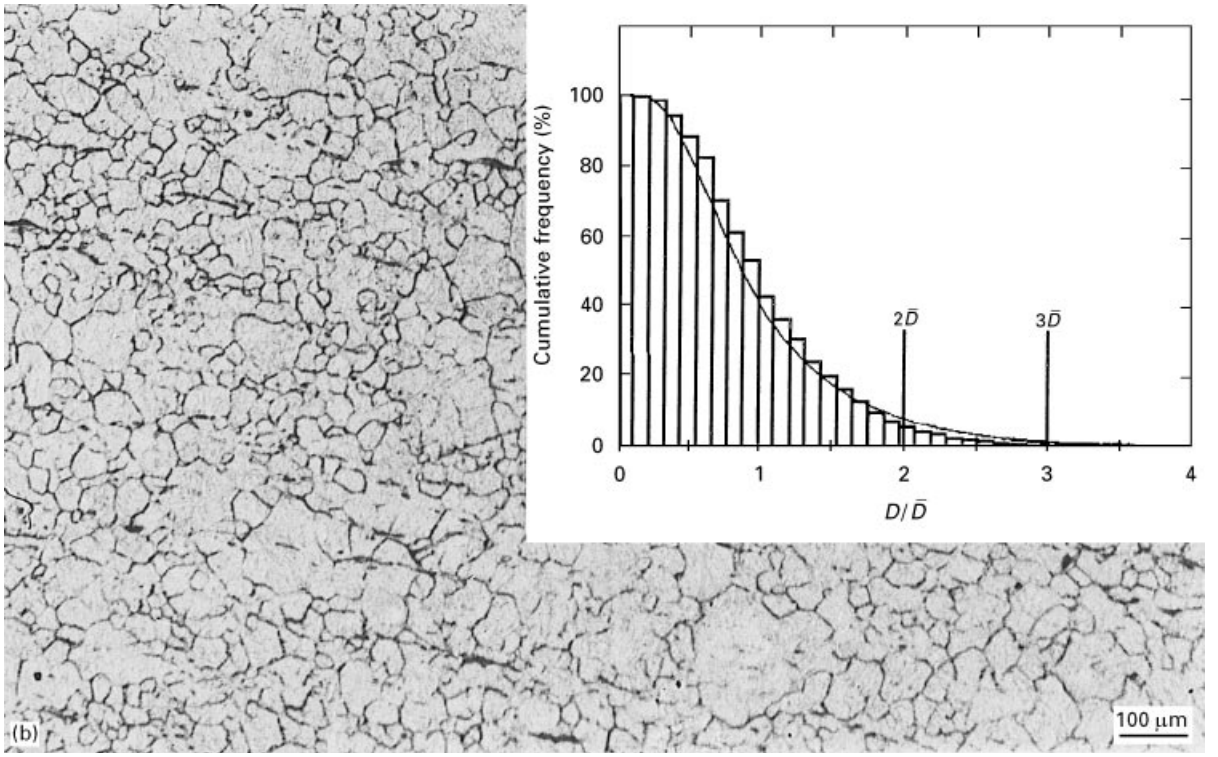

Figure 4 (a) Microstructure and initial grain-size distribution obtained on annealing the sample at 1123 K for 5 min. (b–d) Microstructure and grain-size distribution of steel annealed at (b) 1273 K for 5 min, (c) 1273 K for 30 min and (d) 1273 K for 400 min.

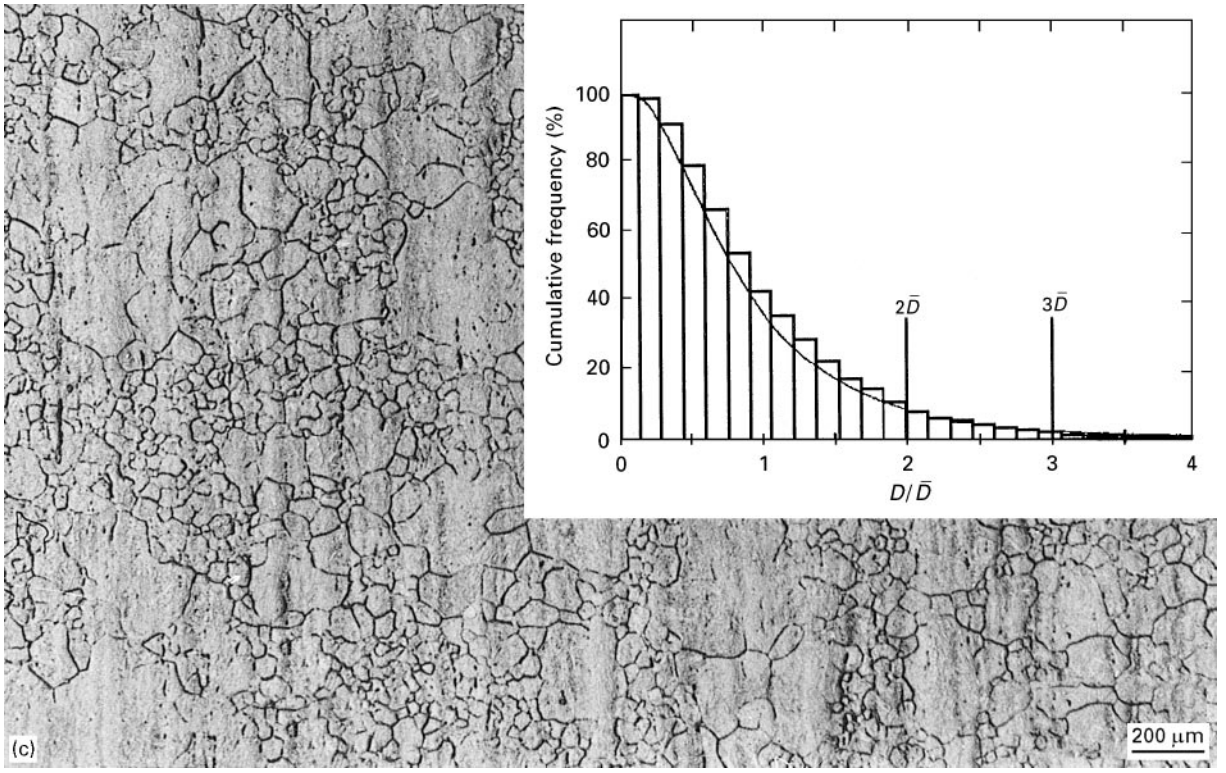

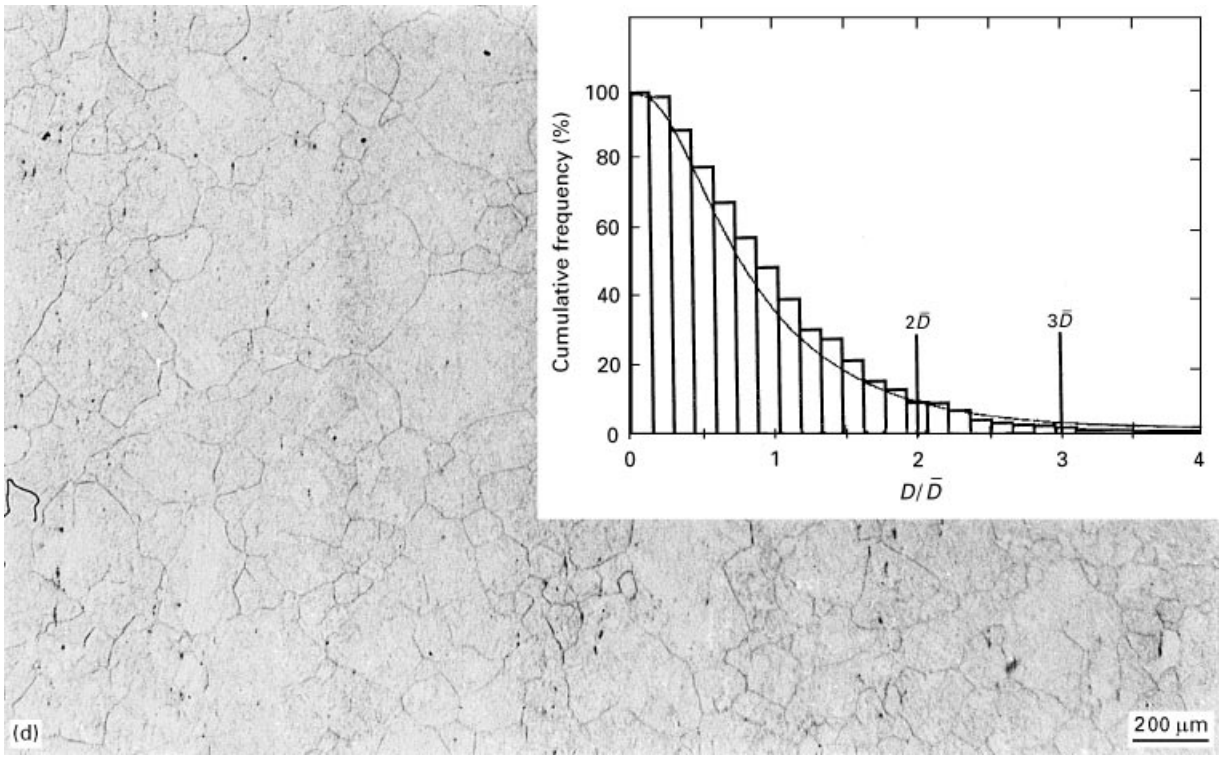

Figure 4 (Continued).

of the original histograms for the calculations. The average rate of grain growth as a function of grain size was calculated by analysis of the cumulative distributions evolution using a methodology described elsewhere [21].

In order to allow comparison with existing normal grain-growth models, the results were normalized following the procedure proposed by Hunderi and Ryum [6]. $v(\rho)$ and ρ were calculated, where v is the normalized grain growth rate; where $\rho = R/R^*(t)$ and R^* is the value of R when $v(\rho) = (dR/dt)/(dR^*/dt) = 0$.

3. Results and discussion

As a result of the microalloying elements, mainly vanadium, the steel developed the fine grained ferrite–pearlite structure shown in Fig. 1.

TEM observations revealed abundant precipitation of the ferrite phase as shown in Fig. 2a. Electron diffraction patterns indicated that precipitates are vanadium carbides of lattice parameter $a = 0.16$ nm, presumably precipitated during cooling after hot rolling and $\gamma \rightarrow \alpha$ transformation; the diffraction pattern of the precipitates is shown in Fig. 2b. Precipitation of

larger particles was also observed, where some of them show characteristic facets (see Fig. 3). EDS measurements revealed that the faceted particles are rich in niobium, which is known to form at temperatures above 1273 K [22]. These particles have been reported to dissolve at higher temperatures, of the order of 1423 K, consistent with a thermodynamic model [23]. The microstructure contains inclusions of manganese sulphide and alumina.

Owing to the fine microstructure and the fine precipitation, the mechanical properties are considerably high. The mechanical properties are yield strength, $\sigma_y = 647$ MPa, ultimate tensile strength, UTS = 902 MPa and 12% for the elongation to the fracture.

Substantial metallographic work had to be done in order to accomplish the observations and measurements described here. A representative set of micrographs was selected to show the microstuctural evolution of the case where annealing was performed at 1273 K. Fig. 4a–d show micrographs of several stages of the austenitic grain structure, including the initial condition (Fig. 4a) and the microstructures after annealing for 5, 30 and 480 min, respectively. Insets show the size distributions in cumulative form that resulted from the line-intercept measurements of the grain structures. The distributions adjust well to the log normal distribution employing a least squares procedure. The microstructure in Fig. 4a and b may be considered normal in the sense that the grains are uniform in size, most of them below two or three times the average size. Abnormal grain growth is apparent in Fig. 4c and d.

The metallographic inspection of the samples of all the heat treatments illustrated in Table II allow the temperature–time diagram of the normal and abnormal grain growth zones to be drawn, as shown in Fig. 5. The grain-growth process is normal at the lower temperature (1173 K) and the abnormality was observed only for the largest annealing time, 480 min. There is a reduced normal grain-growth field at 1273 K, where abnormal grain growth is observed in the samples annealed for longer than 30 min. At 1373 K, abnormal grain growth is observed in the samples annealed for 2 and 3 min. Longer annealing time at this temperature produced normal grain growth.

The grain-growth rate as a function of the grain size which was obtained employing the mean values for grain size at each temperature, is illustrated in Fig. 6. The three curves show that the absolute grain-growth rate is larger in the smaller grains. The abnormality of grain growth at 1273 K is apparent near the second maximum of the growth rate in Fig. 6b. Employing the standard equation, $D = D_0 + kt^n$, a calculation can be made of the value of n at each temperature. The calculated n behaviour is contrary to that reported by other authors [24]. In this case, n drops as temperature increases, as shown in Table III. The different n values have been correlated with changes in the grain-growth mechanism [25]. In

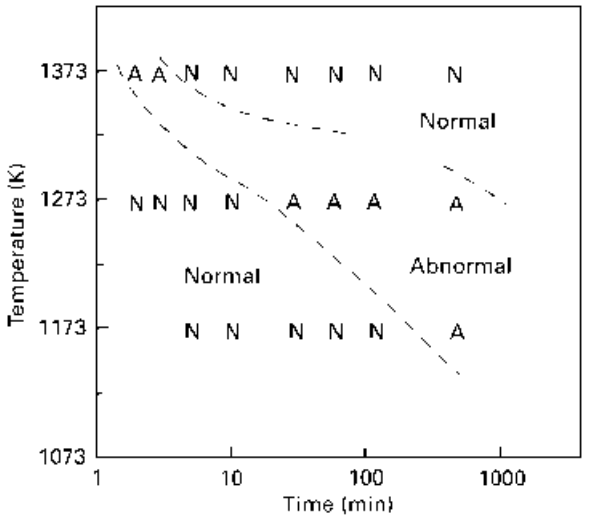

Figure 5 Diagram of normal and abnormal grain-growth zones.

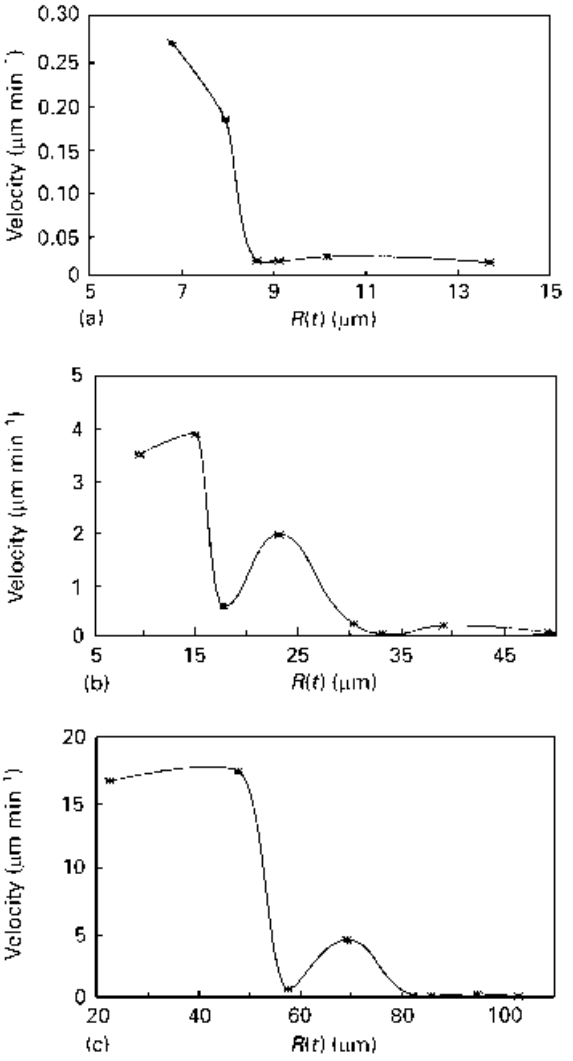

Figure 6 Grain-growth rates calculated from experimental results: (a) 1173 K, (b) 1273 K, (c) 1373 K.

TABLE III Adjustment to kinetic law, $D = D_0 + kt^n$

Temperature (K)	D_0 (μm)	k	n	r^a
1173	6.15	0.7284	0.407	0.96
1273	6.15	7.4477	0.330	0.92
1373	6.15	39.375	0.174	0.81

[a] r = correlation coefficient.

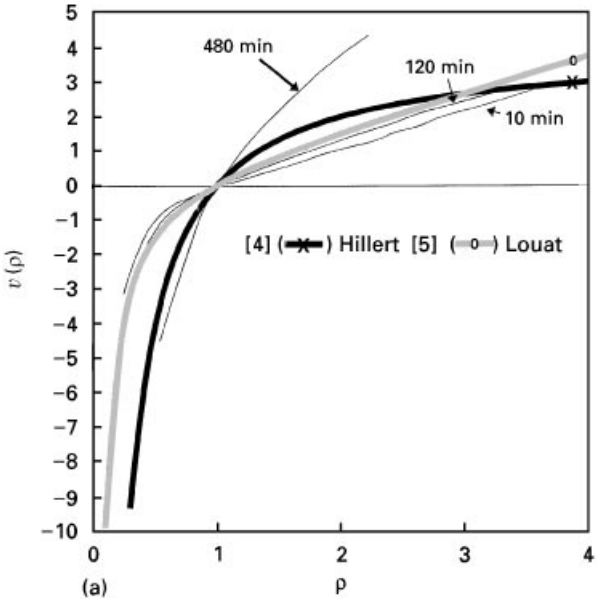

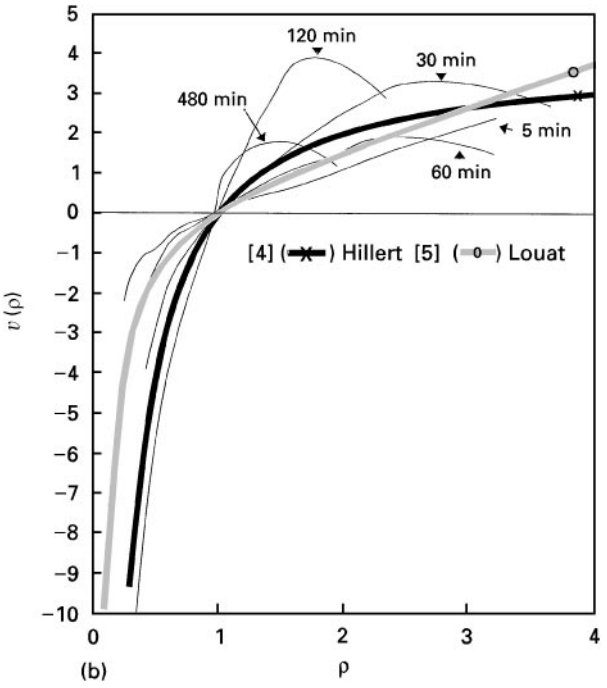

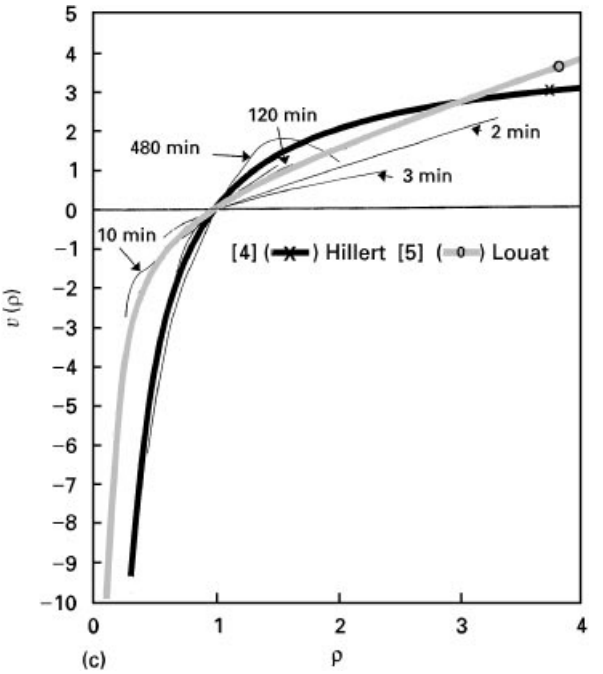

Figure 7 Comparison of normalized experimental results at (a) 1173 K, (b) 1273 K and (c) 1373 K, and normal grain-growth models [3–5].

this case, the dissolution of precipitates modified the pinning condition and, therefore, the grain-growth mechanism.

In order to compare our experimental results with existing grain-growth models, we normalized grain size as $\rho = r/r_{av}$ and grain-growth rate $v = \nu(r)/\nu_{av}$ where v is the normalized grain growth rate; ν is the grain growth rate as a function of grain size r and ν_{av} is the average grain growth rate. Fig. 7a–c compare the normalized experimental results and Hillert and Louat's normal grain-growth models [4–6]. In these graphs, only representative curves are illustrated. At 1173 K in the Fig. 7a, the grain growth is normal almost all the time, except for the curve of 480 min, where the grain-growth rate is larger than at shorter times. This observation coincides well with inspection of the micrographs. At 1273 K (see Fig. 7b), the curves from our experimental results are more separated from the model predictions. Nevertheless, it is possible to distinguish the annealing times for abnormal grain growth. At 1373 K the experimental curves are closer to the predictions of the normal grain-growth models, see Fig. 7c. This comparison with Hillert and Louat's models did not allow the time of the transition of normal grain growth to abnormal grain growth to be obtained. However, in Fig. 7a–c, the fitting to the normal grain models is satisfactory. The normal grain-growth models establish normality lanes, but transition zones should exist between normal and abnormal grain-growth modes. These modes have been treated by Rios [14]. Our results were also compared with the grain-growth map generated by Rios, and it was found that, in general, they coincide well. The results are illustrated in Table IV.

TABLE IV Comparison between experimental (E) and theoretical (T) results. N = normal grain growth; A = abnormal grain growth

Temperature	1173 K		1273 K		1373 K	
Time (min)	E	T	E	T	E	T
2	–	–	N	N	N–A	A
3	–	–	N	N	N	A
5	N	N	N–A	N	N	N
10	N–A	N	A–N	N	N	N
30	N–A	N	A–N	A	N	N
60	N	N	N–A	A	N–A	N
120	N	N	N–A	A	N–A	N
480	A–N	A	N–A	A	N	N

4. Conclusions

A time–temperature map of the normal and abnormal grain-growth modes of the austenite phase of the V–Nb microalloyed steel was built. The map construction

was based on analysis of grain-morphology observations and by extensive line-intercept measurements and calculations which resulted in the time evolution of the grain-size distributions at each temperature. The calculation also yielded the grain-growth velocity as a function of time. The grain-growth behaviour in the temperature interval between 1173 and 1373 K exhibits clear areas of normal and abnormal growth modes. In the time–temperature map, at lower temperatures (1173 K), the grain-growth mode is mainly normal, with a deviation to abnormality only at the longer times. At intermediate temperatures (1273 K), the abnormality region is expanded due to the dissolution of the small vanadium-rich precipitates.

At higher temperatures (1373 K), because most of the precipitated microalloyed steel is already dissolved, the grain-growth mode is mainly normal. A reasonably good agreement resulted from the comparison of the present experimental observations with the theoretical predictions of Rios [14].

Acknowledgements

Authors acknowledge the technical support by A. Gonzalez and J.L. Albarran. O. Flores thanks CONACYT, Mexico, for the support of a scholarship, and L. Martinez acknowledges the support of the J.S. Guggenheim Foundation. This work was supported by CONACYT-UNAM, grant 3878A.

References

1. R. W. CAHN, P. HANSEN and E. J. KRAMER (eds), (Materials Science and Technology, "Processing of Metals and Alloys", Vol. 15 Basel, Cambridge, New York, 1991) p. 371.
2. L. MARTINEZ, *J. Min. Met. Mater. Soc.* **44**(9) (1992) 15.
3. P. FELTHAM, *Acta Metall.* **5** (1957) 97.
4. M. HILLERT, *ibid.* **13** (1965) 227.
5. N. P. LOUAT, *ibid.* **22** (1974) 721.
6. O.HUNDERI and N. RYUM, *J. Mater. Sci.* **15** (1980) 1104.
7. M. P. ANDERSON, D. J. SROLOVITZ, G. S. GREST and P. S. SAHNI, *Acta Metall* **32** (1984) 783.
8. D. J. SROLOVITZ, G. S. GREST and M. P. ANDERSON, *ibid.* **33** (1985) 2233.
9. A. D. ROLLET, D. J. SROLOVITZ and M. P. ANDERSON, *ibid.* **37** (1989) 1227.
10. M. F. ASHBY and K. E. EASTERLING, *ibid.* **30** (1982) 1969.
11. B. RALPH, *Mater. Sci. Technol.* **6** (1990) 1139.
12. H. ADRIAN and F. B. PICKERING, *ibid.* **7** (1990) 176.
13. T. GLADMAN, *J. Min. Met. Mater. Soc.* **44**(9) (1992) 21.
14. P. R. RIOS, *Acta Metall.* **35** (1987) 2805.
15. O. HUNDERI and N. RYUM, *ibid.* **30** (1982) 739.
16. G. ABBRUZZESE, *ibid.* **33** (1985) 1329.
17. C, H, WÖRNER and P. M. HAZZLEDINE, *J. Min. Met. Mater. Soc.* **44**(9) (1992) 16.
18. L. J. CUDDY and J. C. RALEY, *Metall. Trans.* **14A** (1983) 1989.
19. C. V. THOMPSON, H. J. FROST and F. SPAEPEN, *Acta Metall.* **35** (1987) 887.
20. G. S. GREST, M. P. ANDERSON, D. J. SROLOVITZ and A. D. ROLLET, *Scripta Metall.* **24** (1990) 661.
21. J.H. SCHNEIBEL and L. MARTINEZ, *Philos. Mag. A* **54** (1986) 489.
22. M. COHEN and S. S. HANSEN, in "Proceedings of an International Conference on HSLA Steels '85". HSLA Steels: Metallurgy and Applications (Beijing, 1985) p. 4.
23. J. G. SPEER, J. R. MICHAEL and S. S. HANSEN, *Metall. Trans.* **18A** (1987) 211.
24. H. HU, *Can. Metal. Q.* **13** (1974) 175.
25. H. V. ATKINSON, *Acta Metall.* **36** (1988) 469.

Received 24 June 1996
and accepted 18 April 1997